J Med Dent Sci 2013; 60: 83–91

Original Article

Changes in the microvascular structure of mucosal squamous cell carcinoma of the esophagus and their significance in tumor progression

Jirawat Swangsri[1)], Yasuaki Nakajima[1)], Kenro Kawada[1)], Yutaka Tokairin[1)], Tomoyoshi Suzuki[1)], Yutaka Miyawaki[1)], Akihiro Hoshino[1)], Takuya Okada[1)], Shunsuke Ota[1)], Tairo Ryotokuji[1)], Naoto Fujiwara[1)], Tetsuro Nishikage[1)], Kagami Nagai[1)], Hiroshi Kawachi[2)] and Tatsuyuki Kawano[1)]

1) Department of Esophageal and General Surgery, Tokyo Medical and Dental University
2) Department of Human Pathology, Tokyo Medical and Dental University

Background: To identify the clinical T stage by endoscopy is a major diagnostic goal for superficial esophageal squamous cell carcinoma (ESCC). The completion of a microvascular morphological study of mucosal lesions is necessary to optimize therapy.
Materials and methods: Images of 197 intra-papillary capillary loops (IPCLs) captured by magnified endoscopy from 15 esophagectomy specimens were studied for their morphological features and IPCL dimensions.
Results: The microvascular morphology was classified into four basic major patterns: 1. spiral loop, 2. wide loop (WL), 3. globular (G) and 4. reticular pattern. The microvascular features and dimensions differed according to the depth of tumor invasion. Especially the mean bundle outline (IPCL diameter) showed significant changes as 20.02, 22.32, and 27.08 μm, respectively, for M1, M2 and M3, respectively (M1:M2 $P < 0.05$, M2:M3 $P < 0.01$).
Conclusions: During tumor stage progression, a high-volume blood demand and cancer cell overgrowth to occupy the laminar propria mucosa (LPM) cause obvious elongation, thickening, branching, irregularity and deformity of the IPCL, which were characteristics of M3 lesions. The results of the present study support and can be applied with the current Japanese classification for improving the diagnostic accuracy, especially to differentiate between M2 and M3 lesions based on the endoscopic findings.

Key words: Diagnostic techniques and procedures, early cancer detection, intrapapillary capillary loop, esophageal cancer, esophagoscopy.

Corresponding Author: Tatsuyuki Kawano
Department of Esophageal and General Surgery, Tokyo Medical and Dental University, 1-5-45 Yushima, Bunkyo-ku, Tokyo, 113-8519, Japan
Tel: +81-3-5803-5252 Fax: +81-3-3817-4126
E-mail: kawano.srg1@tmd.ac.jp
Received March 15 ; Accepted September 13, 2013

Introduction

Esophageal cancer is the eighth most common cancer worldwide[1]. In 2008, 9,973 cases of esophageal cancer were registered in Japan. Out of the 3,456 total cases of superficial esophageal squamous cell carcinoma (ESCC) 1,705 underwent endoscopic treatment[2]. Esophageal cancer is also an important disease in the USA, where it is the fourth leading cause of death due to GI cancer in male patients[3]. The trend of diagnosing early stage cancer will increase when screening protocols are extended worldwide.

A major way to improve the life expectancy of esophageal cancer patients is to ensure the early detection of cancer, particularly mucosal lesions[2]. The depth of tumor invasion of superficial ESCC is important when determining the therapeutic strategy, and the tumor invasion is categorized in M1 (epthelium), M2 (lamina propria mucosa), M3 (muscularis mucosa), SM1 (superficial subumucosa), SM2 (middle submucosa) and SM3 (deep subumucosa)[2]. The most important staging-related characteristic on the tumor surface is the microvascular pattern. Many pathological studies have found that the microvascular density (MVD) correlates with the disease progression, tumor size, stage and depth of invasion[4-10]. The expression of endothelial regulators such as vascular endothelial growth factor (VEGF) and thymidine phosphorylase is related to the

presence of submucosal tumors and muscularis propria invasion[7,11-15]. High concentrations of cyclo-oxygenase-2 induce inflammatory and angiogenic prostaglandins, and are significantly associated with p53 mutations in the tumor[16]. HER2 over expression is involved in the upregulation of VEGF in various types of tumor cells *in vitro*[17]. The consequences of these changes correlate with the evolution of the tumor microvascular changes.

Magnified endoscopy allows the microvascular features of superficial ESCC to be observed, and intensive studies of these features are needed. After a report describing the intra-papillary capillary loop (IPCL) of the intact squamous mucosa was published by Inoue et al.[18], the endoscopic finding of a microvascular pattern of superficial ESCC became an important issue, and it was found to be related to the microvascular dynamics, tumor progression and lymphatic involvement[18-20]. Because lymphatic involvement is extremely rare in M1 and M2 lesions, endoscopic discrimination between M2 and M3 lesions will impact clinical practice. Although all patients with M1 and M2 ESCC can be cured by endoscopic resection such as endoscopic mucosal resection (EMR) or endoscopic submucosal dissection (ESD), in patients with M3 ESCC the possibility of latent lymph node metastasis should always be considered.

Even though microvascular classifications for superficial ESCC were proposed more than a decade ago[18-20], the completion of the data to make a precise diagnosis continues to be necessary. The aim of this study was to explore the systematic evaluation of the microvascular features of mucosal ESCC (M1-M3), by correlating the morphological observations and a dimensional analysis with pathological data. All of the data will contribute to a better understanding and precise diagnosis of the tumor invasion of superficial ESCC from the aspect of microvascular changes.

Materials and methods

Specimens from both thoracotomy and thoracoscopic esophagectomy obtained from April 2010 until April 2012 that totally or partially included superficial ESCC were evaluated in this study. The patients who received neoadjuvant chemo-radio therapy or had previously undergone therapeutic endoscopy before the operation were excluded. Out of 17 cases that underwent esophagectomy, two were excluded because the specimen was unavailable in one case and because of the undifferentiated cell type in another case. Ten points from a total of 66 magnified endoscopic study points that had a suboptimal microvascular appearance, special pathological type and suspected tissue trauma were also excluded from the analyses (Fig. 1). All IPCL-like microvessels in the cancerous area were called IPCL in this study for expendiency. Nine normal IPCL units from three magnified endoscopic points and 197 malignant IPCL units from 56 points (17, 28, and 11 points were of M1, M2 and M3 grades, respectively) were studied.

The endoscopic phase of a magnified endoscopy system, the Fujinon FTS EG590ZW was used as a standard observational device (the highest magnification covered an endoscopic visual field 1.7 mm in diameter, which was displayed on a 30 cm horizontal monitor, which created ~80x-170x magnification power on the endoscopic monitor). The lesion was observed entirely and the area of optimal appearance of the microvascular structure was inspected precisely up to the highest magnification power. The endoscopic data were recorded as both still pictures and movie files. After the data review, the iodine-stained specimen's image was marked to determine the pathological cutting

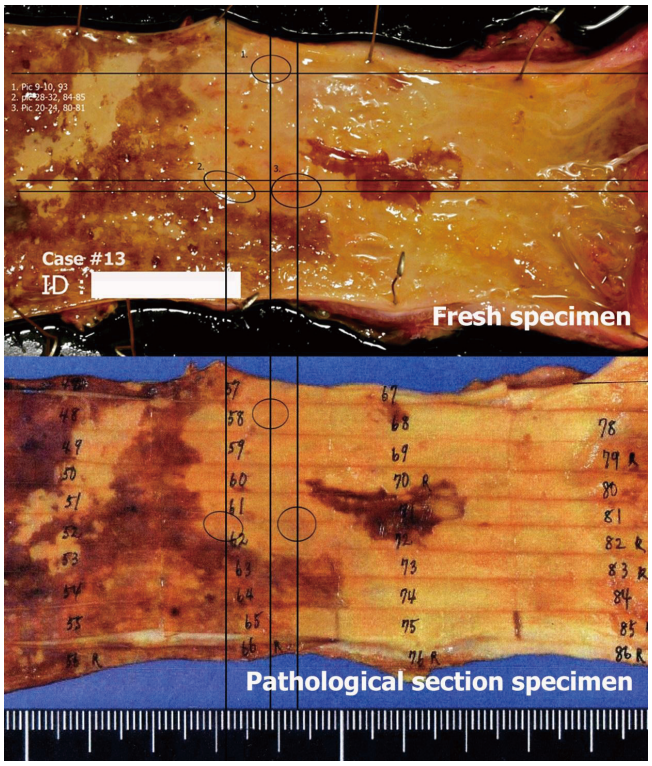

Fig. 1. The inspection point was marked on the image of the specimen to determine the pathological section line.
The image was also useful for selecting the pathological slide, and the landmarks accurately indicated the pathological microscopic location related to the endoscopic inspection point.

line with regard to the specific endoscopic inspection point (Fig. 1).

The pathological phase began with cutting the fresh specimen along the inspection point of the marked images (Fig. 1). The pathological slides were interpreted by a qualified pathologist according to the Japanese Classification of Esophageal Cancer[21,22] and the WHO Classification of Tumors of the Digestive System[23]. The pathological sections were reviewed, and assessment of the tumor stage, thickness and differentiation were collected as data.

The data collection and analysis from the magnified endoscopic findings were examined in relation to the pathological findings. The features of the microvessel unit were considered on the basis of the principle IPCL structure, which comprises four major components: the inflow tract, pedicle, loop, and outflow tract (Fig. 2). For the statistical analysis of the IPCL dimension, the endoscopic images were post-process resolution optimized and the IPCL calibers were visualized via general endoscopy (visual IPCL diameter, called the "bundle outline") compounded from the smallest capillary microvascular (MV) unit. Therefore, the major parameters for the collecting data were: the MV diameter, bundle outline, loop diameter (or width of the globular and reticular pattern), IPCL length (longest dimension of the IPCL) and area (area occupied by one IPCL unit or one circular area with a reticular pattern), which were measured by the Analyzing Digital Images software program in micrometers (μm) and square micrometer (μm^2) units (Fig. 2). The evaluation of the homogeneity of IPCLs was made based on the regularity of IPCL shape in the same observation point.

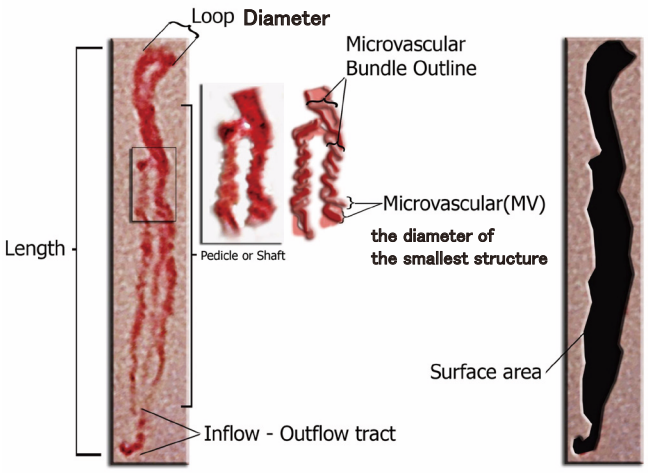

Fig. 2. The structures of the intra-papillary capillary loop (IPCL) unit were divided into four major parts: 1. the inflow tract, 2. the pedicle, 3. the loop and 4. the outflow tract.
The parameters measured for the data analysis were, microvascular (MV): the diameter of the smallest structure compound that could be possible capillary vessels or an indicator of RBC stasis; the bundle outline: the smallest structure which could be visualized by non-magnified endoscopy equal to the IPCL diameter; the loop diameter: the U-turn part or tip of each IPCL unit, or the width of the globular and reticular pattern; the length: the longest dimension of the IPCL unit, and the area: the surface area which was covered by one IPCL unit or one circle of the reticular pattern. The MV, outline, loop and length were recorded in micrometers (μm) and the area was recorded in square micrometers (μm^2).

A statistical analysis was performed using the IBM SPSS software program version 20 for one sample t-tests, independent sample t-tests and a one-way ANOVA. The applied statistical analyses were one sample T-tests to calculate the mean and range (95%CI) of each parameter, independent T tests for comparisons of the parameters of two subjects (for the IPCL classifications which included only two types, e.g. the bundle outline of G-M2 and G-M3), and an ANOVA to compare parameters of three subjects, e.g. the bundle outline of SL-M1, SL-M2 and SL-M3. Normal IPCLs were excluded from the statistical comparing analyses because normal IPCLs are well known to be quite different from cancerous IPCLs[18-20].

The study protocol (No. 1375) was approved by the Human Ethics Review Committee of Tokyo Medical and Dental University, and a signed consent form was obtained from each patient.

Results

Normal mucosa showed a thin IPCL, which was compounded from the smallest MV unit, which twisted and twirled internally and between the bundles to form an almost helical structure, with the tip forming a U-turn loop (Fig. 3).

The IPCL morphology of the mucosal ESCC could be categorized into four major patterns: a spiral loop (SpL), wide loop (WL), globular (G) and reticular (R) pattern. The SpL pattern could be further divided into a simple loop (SL) and complex loop (CL). The R pattern could also be classified into two different structures, the single reticular (SR) and complex reticular (CR) pattern (Fig. 4). The frequency of the detection of each IPCL pattern by observational points was 9/56 (16%), 24/56 (42.9%), 10/56 (17.8%), 5/56 (8.9%), 5/56 (8.9%) and 3/56 (5.4%), respectively, for the SL, CL, WL, G, SR and CR patterns.

The measured data of each parameter are shown in Table 1. In addition, the data regarding the bundle outline, which were the most characteristic findings in

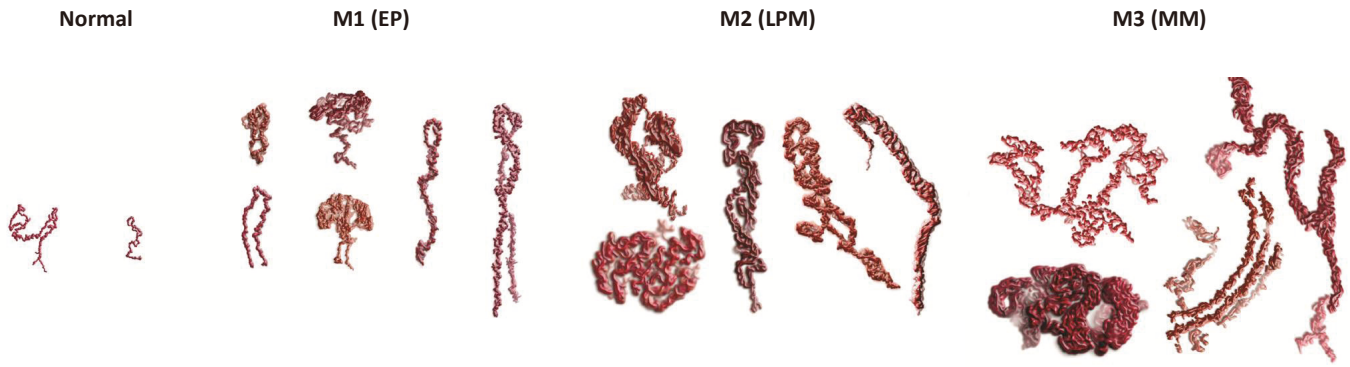

Fig. 3. An illustration of the various features of IPCL evolution from normal mucosa, M1, M2 and M3 lesions.
a: The IPCL of normal mucosa has a very thin bundle outline and a very small area,
b: The IPCL of M1 (EP) lesions is characterized by thin bundle outlines and cover a small area,
c: The IPCL of M2 (LPM) lesions is characterize by a thick bundle outline with a slightly irregular shape with a little branching,
d: The IPCL of M3 (MM) lesions is characterized by a thickened bundle outline with an irregular shape with branching.
These figures demonstrate the variety of shapes which increase in irregularity, complexity and dimension with the progression of staging. They also demonstrate the bundle outline of the IPCL composed of the MV microstructure.

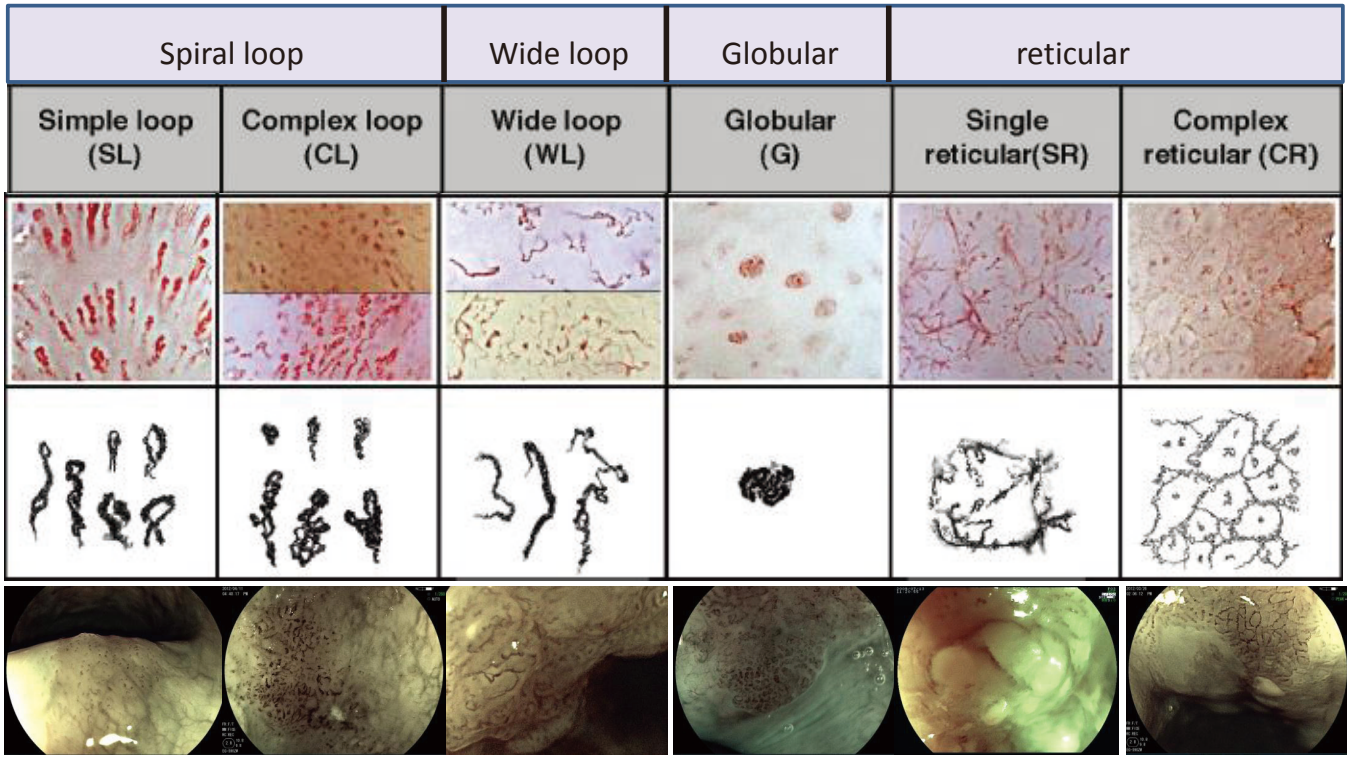

Fig. 4. A summary of the microvascular pattern of the IPCL of superficial ESCC (M1-M3) based on the morphological appearance.
This table contains images of pathological section, magnified endoscopic images and a schematic diagram of the microvasculature. The IPCL can be divided into four major patterns: spiral loop (divided into a simple loop [SL] and complex loop [CL]), wide loop (WL), globular (G), and a reticular pattern (divided into a single reticular [SR] and complex reticular [CR] pattern). This can also suggest the level of tumor differentiation and thickness.

Table 1. Comparison of microvascular structural dimension of each pattern between normal mucosa, M1, M2 and M3. N/A : non available *due to inappropriate value, **due to inadequate data value. Significance : p - value < 0.05, highly significance : P - value < 0.01.

Parameter	n 197 units	MV (μm) mean (95%CI)	Bundle outline (μm) mean (95%CI)	Loop (μm) mean (95%CI)	Length (μm) mean (95%CI)	Area ($μm^2$) mean (95%CI)	Tumor thickness mean (95%CI)
Normal	9	4.91 (4.23-5.59)	8.59 (5.09-12.10)	34.45 (32.68-36.21)	92.76 (80.27-105.24)	2228.6 (1953.83-2519.09)	-
SL-M1	15	6.15 (5.57-6.72)	18.25 (16.65-19.84)	46.84 (41.23-52.456)	195.99 (107.79-284.19)	5700.07 (3430.63-7969.49)	150
SL-M2	35	6.37 (6.07-6.66)	22.75 (20.94-24.55)	64.54 (57.48-71.59)	202.85 (182.71-222.99)	8706.51 (7178.09-10234.94)	259.25
p-value	M1-M2	0.451	< 0.01	< 0.01	0.824	< 0.05	< 0.01
CL-M1	22	5.64 (5.25-6.04)	20.96 (18.47-23.45)	63.38 (54.97-71.79)	127.38 (97.55-157.22)	5070.78 (3673.60-6467.96)	105.35
CL-M2	30	6.55 (6.28-6.82)	21.82 (19.71-23.93)	57.48 (50.25-64.70)	169.25 (137.73-200.76)	6690.8 (5257.79-8123.80)	400 (339.36-380.63)
CL-M3	21	6.69 (6.01-7.39)	27.08 (23.81-30.35)	83.02 (47.08-118.98)	233.39 (176.07-290.72)	13518.14 (8288.34-18747.95)	714.28 (582.52-846.04)
p-value	M1-M2, M2-M3	< 0.01, 0.645	0.61, < 0.01	N/A*, < 0.05	0.097, < 0.05	0.361, < 0.05	< 0.01, < 0.01
WL-M2	13	7.68 (7.01-8.35)	20.6 (17.41-23.81)	40.49 (19.70-61.29)	208.78 (150.05-267.51)	13081.77 (6634.18-19529.35)	515.38 (500.87-529.89)
WL-M3	14	7.77 (6.89-8.64)	25.13 (18.54-31.72)	58.71 (47.99-69.43)	295.83 (213.67-377.99)	15248.5 (6708.75-23788.24)	750 (500.88-999.11)
p-value	M2-M3	0.868	0.204	0.063	0.077	0.668	0.062
G-M2	13	6.62 (6.31-6.92)	23.81 (20.35-27.26)	95.18 (78.91-111.44)	182.37 (148.61-216.13)	16427.61 (11325.91-21529.32)	330.77 (238.01-423.52)
G-M3	1	7.97 (6.22-9.71)	36.7 (28.79-44.61)	169.5	307.3	44053.5	500
p-value	M2-M3	0.095	< 0.01	N/A**	N/A**	N/A**	N/A**
SR-M1	1	4.79 (4.52-5.07)	14.97 (13.01-16.93)	447	477	147188.17	60
SR-M2	5	5.63 (5.45-5.81)	16.98 (16.03-17.93)	410.61 (397.31-423.92)	551.29 (541.04-561.55)	160301.59 (154426.33-166176.86)	311.18 (299.09-323.27)
SR-M2	1	6.08 (5.82-6.34)	27.22 (24.24-30.21)	457	864	177415.39	750
p-value	M1-M2, M2-M3	< 0.01, < 0.05	0.135, < 0.01	N/A**, N/A**	N/A**, N/A**	N/A**, N/A**	N/A**, N/A**
CR-M1	5	4.79 (4.43-5.14)	15.04 (14.11-15.97)	275.3 (263.74-286.86)	379.35 (371.37-387.32)	66817.5 (63795.79-69839.22)	150
CR-M2	7	5.52 (5.16-5.88)	17.42 (15.15-19.67)	211.38 (201.78-220.97)	336.15 (321.36-359.94)	56806.76 (51045.91-62567.61)	400
CR-M2	5	6.64 (6.51-6.78)	18.38 (17.45-19.32)	339.24 (328.29-350.19)	509.98 (489.07-530.89)	140494.16 (131476.20-149512.11)	1100
p-value	M1-M2, M2-M3	< 0.05, < 0.05	0.082, 0.417	N/A*, < 0.01	N/A*, < 0.01	N/A*, < 0.01	N/A**

this study, are described in the results regarding the IPCL patterns.

This study identified the IPCL pattern by starting with the abbreviation of the IPCL type, followed by the tumor depth, e.g. a simple loop M1 lesion was called SL-M1.

The spiral loop pattern

This spiral loop pattern was the most common for all depths, and the major microvascular characteristic was an internal twirling of each bundle and possibly a twisting together of the inflow and outflow tracts at the pedicle. One type of spiral loop had a simple U-curve at

Table 2. The frequency of IPCL pattern (units) in each depth of invasion

	Spiral loop		Wide loop	Globular	Reticular	
	SL	CL			SR	CR
T1a-EP (M1)	15 (30%)	22 (30%)	0	0	1 (14%)	5 (29%)
T1a-LPM (M2)	35 (70%)	30 (41%)	13 (48%)	13 (93%)	5 (71%)	7 (41%)
T1a-MM (M3)	0	21 (29%)	14 (52%)	1 (7%)	1 (14%)	5 (29%)
Total	50	73	27	14	7	17

Table 3. A comparison of the dimensions between the normal mucosa and lesions with the spiral IPCL (SL+CL) pattern.

	n	MV (μm)	Bundle outline (μm)	Loop (μm)	Length (μm)	Area (μm^2)	Tumor thickness (μm)
Normal mean (95%CI)	9	4.91 (4.23-5.59)	8.59 (5.09-12.10)	34.45 (32.68-36.21)	92.76 (80.27-105.25)	2236.49 (1953.83-2519.09)	
M1 mean (95%CI)	37	5.82 (5.50-6.14)	20.02 (18.30-21.73)	57.61 (51.46-63.77)	151.32 (115.75-186.89)	5290.3 (4137.29-6443.31)	113.23
M2 mean (95%CI)	65	6.45 (6.25-6.65)	22.32 (20.98-23.66)	61.28 (56.28-66.27)	187.34 (169.24-205.45)	7776.18 (6718.61-8833.75)	307.69
M3 mean (95%CI)	21	6.7 (6.01-7.39)	27.08 (23.81-30.34)	83.03 (47.07-118.98)	233.39 (176.07-290.72)	13518.14 (8288.33-18747.95)	714.28
p-value	M1-M2	< 0.05	< 0.05	0.599	0.057	< 0.05	< 0.01
	M2-M3	0.34	< 0.01	< 0.01	0.057	< 0.01	< 0.01

the tip, and was called the SL type, while another type appeared to have a more complicated U-turn loop. This type was called a CL type pattern (Fig. 4).

The frequency of the IPCL patterns (units) for each depth of invasion is shown in Table 2. And the SL type was found only in M1 and M2 lesions. The mean (95%CI) bundle outlines were 18.25 (16.65 - 19.84) and 22.75 (20.94 - 24.55) μm ($P < 0.05$) for SL-M1 and SL-M2 lesions, respectively (Table 1).

The CL structure was found in M1, M2 and M3 lesions, but differed in detailed appearance such as thickness and complexity based on the depth. In the macroscopic view, its features had a dotted-like appearance or a mushroom-like appearance. In the CL-M3 lesions, the IPCL was a more complex irregular loop with branching, and the overall size was larger than that of CL-M1 and CL-M2 lesions. The mean (95%CI) bundle outlines were 20.96 (18.47 - 23.45), 21.82 (19.71 - 23.93), and 27.08 (23.81 - 30.35) μm (M1 - M2: $P = 0.61$, M2 - M3: $P < 0.01$) respectively for CL-M1, CL-M2 and CL-M3 (Table 1, Fig. 4).

Comparing the parameters between the IPCL of the normal mucosa and the spiral loop (SL + CL) showed that the mean (95%CI) bundle outlines were 8.59 (5.09 - 12.10), 20.02 (18.30 - 21.73), 22.32 (20.98 - 23.66), and 27.08 (23.81 - 30.34) μm, respectively, for the normal, M1, M2, and M3 mucosa (Table 3).

Table 4. Comparison of the IPCL homogeneity at the observed points between M1, M2 and M3 lesions.

		Homogeneous	Inhomogeneous
M1	16	9 (56%)	7 (44%)
M2	29	13 (45%)	16 (55%)
M3	1	1 (9%)	10 (91%)

The wide loop pattern

This characteristic patternof the microvascular appearance was associated with stretching of the IPCL, and the inflow-outflow tracts were widely separated. Wide loops were generally found in M2 and M3 lesions. WL-M3 lesions presented more complicated branching than WL-M2 lesions, and sometimes seemed to have multiple layers of wide loops. The mean (95%CI) bundle outlines were 20.6 (17.41 - 23.81) and 25.13 (18.54 - 31.72) μm, respectively for WL-M2 and WL-M3 lesions (Table 1, Fig. 4).

The globular pattern

This globular pattern was also mainly found in M2 and M3 stage lesions, especially in M2 disease. This type was composed of multiple microvascular bundles in a

globular shape without any clear regions of inflow or outflow. The mean (95%CI) bundle outlines were 23.81 (20.35 - 27.26) and 36.70 (28.79 - 44.60) μm ($P < 0.05$), respectively, for G-M2 and G-M3 lesions (Table 1, Fig. 4).

The reticular pattern

The reticular pattern could be recognized as two different sub-patterns, the single reticular (SR) and complex reticular (CR) patterns, both of which could be found in M1, M2 and M3 lesions.

The SR type was characterized by circular microvascular complex, which was like a compound of multiple non-uniform IPCL braids that seemed to form a single unit. In SR-M2, the circle complex was larger than that of SR-M1 lesions, with internal and external branching, and the bundle outlines were somewhat thicker than those of SR-M1 lesions. The mean (95%CI) bundle outlines were 14.97 (13.01 - 16.93), 16.98 (16.03 - 17.93) and 27.22 (24.24 - 30.21) μm (M1:M2 $P = 0.27$, M2:M3 $P < 0.05$) for SR-M1, SR-M2 and SR-M3, respectively (Table 1, Fig. 4).

The complex reticular (CR) pattern was also detected in M1, M2 and M3 lesions. The characteristic pattern was a multi-circle complex with sharing of the circle wall between neighboring circles. CR-M2 lesions had central IPCL and a circular wall which was also simple, but significantly thicker than CR-M1. CR-M3 lesions showed pathognomonic internal septation and multiple branching. The mean (95%CI) bundle outlines were 15.04 (14.11 - 15.97), 17.42 (15.15 - 19.67), and 18.38 (17.45 - 19.32) μm for CR-M1, CR-M2, and CR-M3 lesions, respectively (Table 1, Fig. 4).

Homogeneity

An observation of the homogeneity showed no obvious relationship with M1 and M2 lesions, while most of the M3 lesions were inhomogeneous in appearance; heterogeneity was observed in 10 patients (91%). The rate of detection of a homogeneous IPCL area in each stage was: 9/16 [56%], 13/29 [45%] and 1/11 [9%] for M1, M2 and M3 lesions, respectively (Table 4).

Discussion

As part of theories underlying the microvascular evolution examined in this study we considered the MV to be the smallest part composing the larger "bundle outline" structure of the IPCL caliber at the general endoscopic level. The bundle outline diameter is similar to the diameter of a normal capillary and red blood cell (7.5 and 8 μm, respectively)[24]. The MV diameter is less important in terms of application for the clinical setting, and may be an artifact or simply an indicator of RBC stasis because the visualized MV structure is unclear with regard to the limitations of endoscopic CCD resolution. During the progression of an M1 lesion, the tumor cell growth occurs in the epithelium without affecting the IPCL shape, while M2 tumor cells show slightly downward growth to the partially occupied LPM where they exert initial effects on the IPCL structure beneath. The bundle outline is significantly enlarged for each stage due to capillary hyperplasia, and some thickening bundle outlines are found as a result of spiral twisting or segmental dilatation. In M3 lesions, the tumor cell overgrowth occupies the LPM space and directly induces the IPCL contour by causing tortuous and irregular growth, while the cancer cells exhibit increases in nutritional demand, encouraging IPCL modification by inducing neovascularization, thus leading to complexity and branching. The results of the present study and the current Japanese classification (proposed by the Japan Esophageal Society, http://esophagus.jp/download/endoscope_classification.html) are similar for the non-reticular pattern regarding the increase in the IPCL diameter (bundle outline) and size (area) according to the stage progression, and were obviously different in the shape between M2 and M3 lesions according to the appearance of neovascularization (B1 and B2). The reticular pattern of this study is comparable to that of the AVA (avascular area) defined in the current Japanese classification; however, it is quite different with respect to the details, such as the dimensions and appearance. In the Japanese classification, the estimated diameter of the AVA unit (0.5, 0.5-3 mm for B1 and B2, respectively) is significantly larger than the diameter of the reticular pattern unit (width [loop] and length average ~ 200 - 500 microns for M1 - M3).

This study is the first to evaluate the IPCLs on a resected specimen, which allows for more intensive inspection than an *in vivo* study. In addition, the cut specimen is suitable for precisely comparing the location with the pathological section. However, there were confounding factors present at many steps in the present study. For example, where tissue preservation is concerned, suboptimal findings, such as inadequate capillary filling or traumatized capillaries were found in some cases, and may have been the result of tissue manipulation during resection, specimen preparation and the duration before inspection. To resolve these problems, it is necessary to treat samples as gently as possible, to avoid squeezing the blood out, and

to perform the studies as soon as possible after preparation.

We have developed a new guideline to illustrate the advantages and applications of the microvascular morphology to indicate the depth of superficial carcinoma invasion. There are two major features regarding the IPCL morphology, leading to specific patterns which include globular and reticular pattern. These patterns express the pathognomonic characteristics specifically related to the tumor depth. The non-specific patterns are SL, CL and WL. If a specific pattern cannot be detected or the findings are equivocal, the overall data should be analyzed to make the clinical diagnosis. The morphology indicated by the microvessel shape, complexity and branching should be considered in combination with dimensional information, such as the bundle outline, length and area (based on the endoscopic findings). By collecting the data about the bundle outline and length, those that are two-fold the normal IPCL and exhibit a simple microvessel shape are likely to be M1 or M2 lesions, while sizes of three-fold or above the normal size and appearance of neovascularization are likely to be M3 lesions.

Even though these diagnostic criteria cover almost all features of IPCL, some errors are unavoidable because tumor growth is a dynamic and continuous process, and the overlapping or equivocal presentation of the microvascular patterns is common between M1 and M2 lesions, although the differences between M2 and M3 lesions are generally large regarding the morphology and dimensions. For the most effective evaluation, using the highest magnification power of magnified endoscopy is recommended, and the entire lesion should be inspected. When the tumor stage is diagnosed, the tumor thickness can be roughly predicted, however, it is still not possible to predict the tumor differentiation.

Conclusion

The microvascular findings of superficial ESCC appear to be unique, and these findings evolve with tumor progression stage by stage, as evidenced by the dimensional measurements and a statistical analysis. The bundle outline and shape of the IPCL are important parameters with regard to superficial cancer stage prediction. Although some details of the results are different, the concept supports and is applicable to the current Japanese classification, particularly for differentiating between M2 - M3 lesions. The M2 lesions are clearly different from M3 lesions, which exhibit obvious irregular thickening, and a tortuous and branching appearance due to LPM invasion and neovascularization. The application of this system will contribute to making appropriate therapeutic decisions and is also feasible for both the detection and follow-up of lesions.

Acknowledgments

The authors thank Associate Prof. Yoichi Kumagai (Digestive Surgery, Saitama Medical College) for helpful suggestons, particularly with respect to the comparison with the current Japanese classification and the discussion of the reliability of the data and its clinical applications.

References

1 Eslick GD. Epidemiology of esophageal cancer. Gastroenterol. Clin. North. Am. 2009; 38: 17-25.
2 Sakata R, Fujii Y, Kuwano H. Thoracic and cardiovascular surgery in Japan during 2008: annual report by The Japanese Association for Thoracic Surgery. Gen. Thorac. Cardiovasc. Surg. 2010; 58: 356-383.
3 Jemal A, Siegel R, Ward E, Hao Y, Xu J, Thun MJ. Cancer statistics, 2009. CA. Cancer. J. Clin. 2009; 59: 225-249.
4 Nakagawa S, Nishimaki T, Suzuki T, et al. Tumor angiogenesis as an independent prognostic factor after extended radical esophagectomy for invasive squamous cell carcinoma of the esophagus. Surgery 2001; 129: 302-308.
5 Takebayashi Y, Natugoe S, Baba M, et al. Angiogenesis in esophageal squamous cell carcinoma. Oncol. Rep. 1998; 5: 401-404.
6 Igarashi M, Dhar DK, Kubota H, et al. The prognostic significance of microvessel density and thymidine phosphorylase expression in squamous cell carcinoma of the esophagus. Cancer 1998; 82: 1225-1232.
7 Kuwano H, Sonoda K, Yasuda M, et al. Tumor invasion and angiogenesis in early esophageal squamous cell carcinoma. J. Surg. Oncol. 1997; 65: 188-193.
8 Tanigawa N, Matsumura M, Amaya H, et al. Tumor vascularity correlates with the prognosis of patients with esophageal squamous cell carcinoma. Cancer 1997; 79: 220-225.
9 Kitadai Y, Haruma K, Tokutomi T, et al. Significance of vessel count and vascular endothelial growth factor in human esophageal carcinomas. Clin. Cancer. Res. 1998; 4: 2195-2200.
10 Takebayashi Y, Aklyama S, Yamada K, et al. Angiogenesis as an unfavorable prognostic factor in human colorectal carcinoma. Cancer 1996; 78(2): 226-231.
11 Koide N, Nishio A, Kono T, et al. Histochemical study of vascular endothelial growth factor in squamous cell carcinoma of the esophagus. Hepatogastroenterology 1999; 46: 952-958.
12 Inoue K, Ozeki Y, Suganuma T, et al. Vascular endothelial

growth factor expression in primary esophageal squamous cell carcinoma. Association with angiogenesis and tumor progression. Cancer 1997; 79: 206-213.
13 Kitadai Y, Amioka T, Haruma K, et al. Clinicopathological significance of vascular endothelial growth factor (VEGF)-C in human esophageal squamous cell carcinomas. Int. J. Cancer. 2001; 93: 662-666.
14 Takebayashi Y, Natsugoe S, Baba M, et al. Thymidine phosphorylase in human esophageal squamous cell carcinoma. Cancer 1999; 85: 282-289.
15 Li Z, Shimada Y, Uchida S et al. TGF-alpha as well as VEGF, PD-ECGF and bFGF contribute to angiogenesis of esophageal squamous cell carcinoma. Int. J. Oncol. 2000; 17: 453-460.
16 Biramijamal F, Allameh A, Mirbod P, et al. Unusual profile and high prevalence of p53 mutations in esophageal squamous cell carcinomas from northern Iran. Cancer. Res. 2001; 61: 3119-3123.
17 Kumar R, Yarmand-Bagheri R. The role of HER2 in angiogenesis. Semin. Oncol. 2001; 28: 27-32
18 Inoue H, Honda T, Nagai K, et al. Ultrahigh magnification endoscopic observation of carcinoma in situ of the esophagus. Dig. Endosc. 1997; 9: 16-18.
19 Kumagai Y, Inoue H, Nagai K, et al. Magnifying endoscopy, stereoscopic microscopy, and the microvascular architecture of superficial esophageal carcinoma. Endoscopy 2002; 34: 369-375.
20 Arima M, Tada M, Arima H. Evaluation of microvascular patterns of superficial esophageal cancers by magnifying endoscopy. Esophagus 2005; 2: 191-197.
21 Fujita H. Japanese classification of esophageal cancer, tenth edition: part I. Esophagus 2009; 6: 1-25.
22 Shimoda T. Japanese classification of esophageal cancer, the 10th edition-Pathological part II-III. Nihon Rinsho 2011; 69: 109-120.
23 Montgomery E, Field JK, Boffetta P, et al. Squamous cell carcinoma of oesophagus. In: Bosman F.T. CF, Hruban R.H., Theise N.D. (Eds). WHO Classification of Tumours of the Digestive Systems 2010;18-24.
24 Lauralee S. Capillaries. In: Human Physiology from Cells to Systems 8th ed. Canada: Yolanda Cossio; 2013: 361-370